CORA Cork Open Research Archive
Cartlann Taighde Oscailte Chorcaí

Title	Switched three dimensional photonic delay line using directly modulated semiconductor lasers for microwave radar processing
Authors	Madamopoulos, Nicholas;Riza, Nabeel A.
Publication date	1996-11-05
Original Citation	Madamopoulos, N. and Riza, N. A. (1996) 'Switched Three Dimensional Photonic Delay Line using Directly Modulated Semiconductor Lasers for Microwave Radar Processing', Proceedings of SPIE, 2845, Radar Processing, Technology, and Applications, SPIE's 1996 International Symposium on Optical Science, Engineering, and Instrumentation, Denver, CO, United States. doi: 10.1117/12.257231
Type of publication	Conference item
Link to publisher's version	10.1117/12.257231
Rights	© 1996 Society of Photo-Optical Instrumentation Engineers (SPIE). One print or electronic copy may be made for personal use only. Systematic reproduction and distribution, duplication of any material in this paper for a fee or for commercial purposes, or modification of the content of the paper are prohibited.
Download date	2026-11-06 15:15:26
Item downloaded from	https://hdl.handle.net/10468/10179

UCC
University College Cork, Ireland
Coláiste na hOllscoile Corcaigh

PROCEEDINGS OF SPIE

SPIEDigitalLibrary.org/conference-proceedings-of-spie

Switched three-dimensional photonic delay line using directly modulated semiconductor lasers for microwave radar processing

Madamopoulos, Nicholas, Riza, Nabeel

Nicholas Madamopoulos, Nabeel A. Riza, "Switched three-dimensional photonic delay line using directly modulated semiconductor lasers for microwave radar processing," Proc. SPIE 2845, Radar Processing, Technology, and Applications, (5 November 1996); doi: 10.1117/12.257231

SPIE.

Event: SPIE's 1996 International Symposium on Optical Science, Engineering, and Instrumentation, 1996, Denver, CO, United States

Downloaded From: https://www.spiedigitallibrary.org/conference-proceedings-of-spie on 07 Jun 2020 Terms of Use: https://www.spiedigitallibrary.org/terms-of-use

Switched Three Dimensional Photonic Delay Line using Directly Modulated Semiconductor Lasers for Microwave Radar Processing

Nicholas Madamopoulos and Nabeel A. Riza
Center for Research and Education in Optics and Lasers (CREOL)
and the Department of Electrical & Computer Engineering
University of Central Florida
P. O. Box 162700, 4000 Central Florida Blvd.,
Orlando FL 32816-2700
email: riza@creol.ucf.edu

ABSTRACT

A 3-bit binary photonic delay line is demonstrated at 1 Ghz using a directly modulated semiconductor laser and remote interconnection fiber-optics. Three types of freespace delay bit geometries are tested for 5.686 ns, 1.667 ns, and 8.83 ps delay bits. This photonic delay line uses ferroelectric liquid crystal optical on/off devices for optical path switching and active polarization noise filtering. Three dimensional imaging optics and antireflection coated optics (for all but 5 components) are successfully used to minimize photonic delay line insertion losses and interchannel crosstalk. The 3-bit system is fully characterized for measured and designed performance.

2. INTRODUCTION

Switched three dimensional (3-D) photonic delay lines (PDLs) have become a key photonics research area in recent years. Application of PDLs in microwave radar signal processing offer some important advantages when compared to all-electronic processors. These advantages include large instantaneous and tunable signal processing bandwidths, and protection from electromagnetic interference (EMI) and electromagnetic pulses (EMP).

Over the past few years we have proposed and demonstrated various reversible switched PDL structures for phased array antenna applications [1-7]. These PDLs are based on two dimensional (2-D) pixelated optical polarization switching arrays, such as nematic liquid crystals (NLCs), ferroelectric liquid crystals (FLCs), multiple quantum well (MQW) devices, or magneto-optic devices. We have successfully demonstrated moderately fast optical switching (e.g., 1 ms) using NLC devices while maintaining high on/off optical isolation (e.g., >35 dB) at both output ports of the switch [8-9]. Low inter-channel electrical crosstalk (e.g., -42 dB) has also been demonstrated when using 3-D imaging optics [10].

For our initial experimental PDL research, we worked with visible, unmodulated light for acquiring appropriate optical alignment experience and procedures, and for high observed (to the PDL builder) accuracy of optical noise, signal, crosstalk, and loss measurements. The current wavelength for high speed analog light modulation phased array antenna applications is in the near infrared band (e.g., 1300 nm), mainly because of recent commercial developments in high performance analog fiber-optic links using near infrared, semiconductor-based optical transmitter and receiver technology. These fiberoptic links are being considered as economical and practical solutions for radio frequency (RF) signal transmission and distribution, particularly for microwave phased array antennas/radars.

In this paper, we demonstrate for the first time, a 3-bit 3-D PDL using a remote 1310 nm fiber-optic directly modulated semiconductor laser link, 3-D imaging optics, FLC devices for high speed optical path switching and active polarization filtering, and infrared anti-reflection (AR) coated optics for insertion loss and interchannel crosstalk suppression. We test the reversible switched PDL at a 1 Ghz fiber-optic link modulation frequency, and the overall laboratory system is fully characterized with respect to the microwave carrier-to-noise ratio, insertion loss, spatial interchannel crosstalk, and time delays.

0-8194-2233-9/96/$6.00

Downloaded From: https://www.spiedigitallibrary.org/conference-proceedings-of-spie on 07 Jun 2020
Terms of Use: https://www.spiedigitallibrary.org/terms-of-use

3. 3-BIT 3-D PDL USING FLC DEVICES, IMAGING, AND REMOTING

The experimental setup of our 3-bit PDL is shown in Fig. 1. A Lasertron model QLINK1-051 microwave fiber-optic transmitter (λ=1310 nm) and receiver are used to form the remote fiber link. The Lasertron transmitter is designed to directly convert RF-modulated electrical signals to optical signals. The modulated light is coupled into the PDL by a single mode fiber which is connected to the transmitter module by a FC-PC fiber-optic connector. A GRIN-lens is connectorized at the other end of the several meters length single-mode fiber, and forms the input port to the PDL. The light power output from this GRIN lens for our system was typically near 1.8 mW.

Our PDL system is based on polarization switching, where switching between the two orthogonal polarizations, i.e., vertical (or s-polarization) and horizontal (or p-polarization), occurs. The light transmitted from the microwave fiber-optic transmitter to the PDL is through a non-polarization maintaining (non-PM) fiber. This makes the polarization of the input light to be in general not linear, mainly because of the randomly induced fiber birefringence due to external factors such as environmental changes. This polarization fluctuation, although varying slowly, would adversely affect the overall system performance, particularly in terms of noise leakage through the FLCs and the cube polarizing beamsplitters (PBSs). In order to overcome this problem, a parallel-rub birefringent-mode NLC device and a polarizer are placed at the input of the PDL system to control the input polarization. The state of polarization of the input light can then be controlled by choosing both the appropriate angle of the NLC molecular director relative to the vertical or horizontal axis, and the NLC cell applied voltage. In this way, the magnitude of the vertical component of the input light can be maximized while minimizing the horizontal component. Then a high extinction ratio polarizer is used to block the unwanted horizontal polarization. From day to day, the input power to our system ranged between 1.20 mW to 1.60 mW, with smaller variations of $\pm$ 0.1 mW obtained during the course of a day.

We choose three different PDL bit architectures for our system to demonstrate ultra-short, moderate, and long time delays [7]. 3-D refractive imaging optics are used within the PDL to minimize interchannel crosstalk [10]. A 4f imaging system is formed to image the input (object plane) of each bit at its output (image plane), where this output is the input for the next bit. In general, f refers to the focal length of the spherical plano-convex lenses used in the PDL.

The first bit is based on the single cube PBS, feedback circular delay path geometry design, and can provide the long time delays (> 5 ns). A 3-D imaging system in the delay path consists of two spherical lenses L2's of focal length f_2=40 cm. The time delay for this first bit is given by

$$\Delta t = \frac{4f_2}{c} + 4\left(n_{TIR}\frac{d_{TIR}}{c} - \frac{d_{TIR}}{n_{TIR}c}\right) + \left(n_{PBS}\frac{d_{PBS}}{c} - \frac{d_{PBS}}{n_{PBS}c}\right), \quad (1)$$

where (n_{TIR}, n_{PBS}) and (d_{TIR},d_{PBS}) are the index of refraction and the side physical size of the (TIR, PBS) pair, respectively. c is the velocity of light in vacuum. For our case, n_{TIR}=n_{PBS} =1.5 and d_{PBS} = d_{TIR}=2.54 cm, and hence the designed time delay from bit 1 is **5.686 ns**.

The second bit is based on the transmissive feed-forward, two cube PBS architecture, and gives the moderate time delay (e.g., < 5 ns) in our 3-bit PDL. For the straight (non-delay) path, the imaging lenses have focal lengths f_3=12.5 cm, and for the delay path the imaging lenses have focal lengths of f_4=25 cm. The expected or designed time delay from the second bit is given by

$$\Delta t = 4\frac{f_4 - f_3}{c}. \quad (2)$$

Downloaded From: https://www.spiedigitallibrary.org/conference-proceedings-of-spie on 07 Jun 2020
Terms of Use: https://www.spiedigitallibrary.org/terms-of-use

For our given design, this is a time delay of **1.667 ns.**

The third bit is a symmetric PDL design that provides the ultra-short time delay (<0.1 ns). The two paths in the bit have the same physical length, and imaging optics using lenses L5 and L6 are deployed to minimize interchannel crosstalk ($f_5 = f_6$). A very short optical path-length difference between the two paths can be introduced by placing two glass plates; one plate in each switched path in the bit. The ultra-short time delay can thus be generated by controlling the relative thickness of the two glass plates. In our experimental case, the two glass plates have thicknesses of d_1=0.635 cm and d_2=0.953 cm for the non-delay and the delay paths, respectively. For bit 3, this ultra-short time delay can be calculated from the expression

$$\Delta t = n[\frac{d_2 - d_1}{c}] - [\frac{d_2 - d_1}{nc}], \quad (3)$$

where n=1.5 is the index of refraction of the glass plates. In our case this delay is calculated at **8.83 ps**.

The optical switches used in the PDL are FLC devices that are based on the electro-optic principle of a switchable half-wave plate (HWP). Each device consists of a thin layer (e.g., < 2 μm) of FLC material sandwiched between two glass plates. The liquid crystal is a uniaxial birefringent medium, with its optic axis oriented parallel to the liquid crystal molecules. The optic axis of FLCs has two preferred directions that are separated by approximately 45°, and can be controlled by the polarity of the applied voltage across the electrodes. Thus, the two states of the FLC device can be selected. The devices are driven with a ±5 V bipolar, DC balanced (i.e., a 10 V_{p-p} square wave) waveform. A +5 V with respect to the reference will place the device in the "off" state, and a -5 V with respect to the reference will place the device in the "on" state [9]. We have recently observed that present-day commercially available FLC devices, when set to their "on" state, do not fully rotate the input polarization by 90°. This leakage noise from FLC devices can deteriorate overall system performance. The use of the active noise filter consisting of a second FLC device and a linear polarizer can suppress this polarization leakage noise. On the other hand, when FLC devices are set in their "off" state, they do not greatly deteriorate the state-of-polarization of the input beam. Thus, we choose to operate the two FLC devices of a bit-module in opposing states, i.e., when for example FLC1 is "on", then FLC2 is "off", and vice versa. This leads to a balancing of the polarization leakage noise between the two settings of a bit-module, and hence light lost due to the active noise reduction filter is approximately the same for both settings.

4. PDL DEMONSTRATION AND SYSTEM ISSUES

The following sections describe experimental data from our 3-bit 3-D PDL, and important system issues related to this data are discussed.

4.1 Insertion Loss

An important issue in our PDL system is the optical losses introduced by the optical components. Our attempt is to use AR coated optical components to minimize the optical losses in the system. We use off-the-shelf optical components that have been AR coated for 1310 nm. Component losses are less than 0.25% for every glass surface, and the reflectivity of the mirrors is greater than 99%. The two lenses (L2) in the delay path of the first bit were without AR coatings because of the current non-availability from commercial sources for our specific design. Our non-AR coated lens pair had measured optical losses of 14% and 16%. Table 1 shows the measured and expected optical losses for each bit and for the entire PDL system. Note that all experimental insertion loss data are less than the expected insertion loss values calculated using manufacturer listed specifications. For bit 2 and bit

Downloaded From: https://www.spiedigitallibrary.org/conference-proceedings-of-spie on 07 Jun 2020
Terms of Use: https://www.spiedigitallibrary.org/terms-of-use

3 modules, the optical insertion losses are ≈1.5 dB, a highly desirable number when using a cascaded N-bit PDL design. Only the bit 1 module showed a higher loss, and there are three reasons for this occurance. First, unlike all the other FLC devices that had a measured transmission loss of ≈16 %, FLC1 used in bit 1 had a measured transmission loss of 26 %. Second, the L2 lens pair has no 1310 nm AR coating, hence an additional ≈ 8 % loss per lens. Third, the polarizer after FLC2 also did not have a 1310 nm AR coating; so another 8 % transmission loss. Thus, unlike bit 2 and 3, bit 1 suffered the higher optical insertion loss due to four un-optimized components. Finally, for the overall PDL, two other components did not have 1310 nm AR coatings. These are the NLC device at the input of the PDL and the last polarizer (after FLC6). Hence, if the five non-AR coated components are also AR coated, the overall PDL will have lower insertion loss than demonstrated in our experiment.

4.2 Interchannel Crosstalk

Interchannel crosstalk is also a significant factor for analyzing overall system performance. Light from one optical channel in our 3-D multichannel PDL system can leak to the adjacent channels and this effect will be translated to interchannel crosstalk or noise in the system. The original beam from the PDL input GRIN-lens was 1.8 mm in diameter, i.e., equal to the GRIN-lens diameter. Fig. 2 shows the optical beam spot at the output image plane of the system, i.e., at the location of the output GRIN-lens. The spot size at the image plane was measured to be approximately 2 mm in diameter. Hence, using our 3-D imaging optics design through the entire PDL, the input beam spreading through free-space and solid-optics propagation was kept at a maximum 10 % beam radius increase. This then leads to minimal light levels outside the output beam diameter of 2 mm, as Fig.2 demonstrates. The interchannel crosstalk was accurately measured with an infrared 2-D detector. Measurements were performed every 1.8 mm in the orthogonal directions, namely, the x and y directions of the center active optical channel. We selected the distance of 1.8 mm because this is the diameter for the commercial GRIN lenses at 1310 nm. Recently, we proposed a compact, high packing density, hexagonal GRIN-lens array geometry design for the 2-D output coupling optics of our multichannel PDL system [12]. This fiber-coupling optics design consists of a 2-D array of GRIN lenses stacked side-by-side and top-to-bottom, with GRIN center-to-center distances of 1.8 mm. Hence, the output port interchannel measurement distance is 1.8 mm. Figure 3 shows the measured interchannel crosstalk for our PDL at the output plane, where data is taken for 11 channels in the x-direction and 11 channels in the y-direction, all relative to the center active optical channel. Because we are using 25.4 mm side cube PBSs, for a 1.8 mm interchannel distance, our PDL can pack about 196 optical channels. A highest -27.47 dB optical crosstalk level was measured for the nearest to center channel in the x-direction. Hence, the highest RF interchannel crosstalk for our experimental PDL was -54.94 dB.

4.3 PDL RF Carrier-to-Noise Ratio Measurements

Other important issues of any PDL system are its carrier-to-noise ratio (C/N) performance, and whether it introduces additional noise to the directed modulated fiber-optic link RF signal. Fig. 4a shows the signal taken directly from the Lasertron microwave fiber-optic link when the transmitter and receiver fiber-optic modules are directly connected with a FC/PC connectorized single mode optical fiber. The transmitter is driven by a 15 dBm, 1 GHz signal from a HP synthesizer. The -28.33 dBm output signal is generated by the Lasertron fiber-optic receiver module. Using a RF spectrum analyzer, a RF noise floor of -131.33 dBm is measured at a 100 kHz offset from the 1 Ghz fiber-optic link modulation frequency, for both when the link is not connected and when it is connected to the PDL. A 1 Khz analyzer resolution bandwidth (RBW) is used. A C/N of 103.00 dB/Hz @ 100 Khz is measured for the link without the PDL (see Fig.4a), while a C/N of 79.34 dB/Hz is measured @ 100 Khz offset when the PDL (setting 3) is connected to the directly modulated fiber-optic link (see Fig.4b). Table 2 shows the C/N for five different settings of the PDL, indicating similar C/N's,

Downloaded From: https://www.spiedigitallibrary.org/conference-proceedings-of-spie on 07 Jun 2020
Terms of Use: https://www.spiedigitallibrary.org/terms-of-use

except for setting 5 of the PDL that incurs higher insertion loss due to four bit 1 unoptimized components. The noise floor of the fiber link-PDL system remains below -130 dBm for all settings of the PDL.

The signal level detected after propagation through the PDL and fiber link is -54.66 dBm, indicating a 26.33 dB PDL RF insertion loss. If we treat the PDL as an attenuator, then an equivalent C/N can be calculated and compared to the original link C/N. This equivalent C/N can be calculated by taking a sum of the measured link-PDL C/N plus the attenuation (or negative gain) of the PDL. In this case, we get 79.34 + 26.33= 105.67 dB/Hz, which is similar to the C/N available form the Lasertron fiber link. Hence, our PDL does essentially act as an attenuator to the microwave fiber-optic link, with minimal link C/N reduction due to increased RF noise.

The measured PDL setting 3 RF insertion loss of 26.33 dB is equivalent to a 13.165 dB optical insertion loss. From Table 1, we note that a 5.5 dB optical insertion loss is measured for the PDL setting 3 from the bit 1 input port (after the polarizer that follows the NLC device) to the bit 3 output port (just before output GRIN). Compared to the direct fiber connection between the fiber-optic transmitter and fiber-optic receiver, the remote fiber link connection to the PDL uses one extra FC/PC connector, a PDL input light polarization controller (PC), and free-space light coupling to the output GRIN-lens. All these items cause the extra 13.165-5.5=7.665 dB optical insertion loss in the system. We measured a 4.3 dB (or 63%) optical insertion loss in the free-space-to-output GRIN-lens coupling optics. Hence, the remaining 7.665-4.3=3.365 dB optical insertion loss occurs due to the PC and the additional FC/PC connector. With proper design, these losses can be greatly reduced.

4.4 Time Delay Measurements

Fig. 5 shows the time delayed signal for three different PDL settings. The top trace shows the signal when light goes through the non-delay setting for all the bits (setting 1). The middle trace is obtained when bit 2 and bit 3 are set for delay and bit 1 for non-delay (setting 4). The designed time delay is 1.667 ns. The delay measured using a Tektronix digital oscilloscope is 1.660 ns (Fig. 5a). The bottom trace is obtained for the PDL setting in which the first bit is set for delay and the other two for non delay (setting 5). The designed time delay was 5.686 ns. The oscilloscope trace measures a time delay of 5.720 ns (Fig. 5b). The slight discrepancy in the designed and measured time delays for our PDL occurs due to the variable and finite manufacturer specified error tolerances of the optical components used in the PDL, plus the measurement errors due to the use of a digital oscilloscope to measure time delays.

5. CONCLUSION

In conclusion, we have demonstrated a 3-bit PDL using FLC devices, imaging optics, and system remoting via a directly modulated 1310 nm semiconductor laser. Very low -54.94 dB RF interchannel crosstalk was measured in the nearest adjacent PDL output channel. Our PDL system essentially does not degrade the C/N of the Lasertron fiber-optic link modulated at 1 Ghz. In essence, our PDL acts as an RF attenuator, providing additional insertion loss to the fiber link-PDL system. PDL measured insertion loss has been characterized indicating that near 1.5 dB optical loss is achievable per bit. Future work includes reducing the FLC device insertion losses, improving output freespace-to-GRIN lens optical coupling efficiency, and replacing the five non-AR coated optical components in our present laboratory PDL with AR coated components.

6.ACKNOWLEDGEMENTS

Support for this work is provided by Grant No.N000149510988 from the Office of Naval Research, program monitor, Dr. W. Miceli.

Downloaded From: https://www.spiedigitallibrary.org/conference-proceedings-of-spie on 07 Jun 2020
Terms of Use: https://www.spiedigitallibrary.org/terms-of-use

7. REFERENCES

[1] N. A. Riza, "Liquid crystal-based optical time delay units for phased array antennas," *IEEE/OSA Journal of Lightwave Technology*, Vol. 12, No. 8, pp. 1440-1447, 1994.

[2] N. A. Riza, "A transmit/receive time delay optical beamforming architecture for phased array antennas," *Applied Optics*, Vol 30, No. 32, pp.4593-4596, 1991.

[3] N. A. Riza, "Liquid crystal-based optical time delay control system for wideband phased arrays," *SPIE Conference on Analog Photonics OE/Fibers*, Vol. 1790, pp. 171-183, 1992.

[4] N. A. Riza, "Three-dimensional optical time delay units for radar," *SPIE Proc.*, Vol. 2026, pp. 227-237, San Diego, 1993.

[5] N. A. Riza, "Polarization-based fiber optic delay lines," *SPIE Conference on Optical Technology for Microwave Applications VII*, Vol. 2560, pp. 120-129, 1995.

[6] N. A. Riza, and N. Madamopoulos, "High signal-to-noise ratio birefringence compensated optical delay line based on a noise reduction scheme," *Optics Letters*, Vol. 20, No. 22, pp. 2351-2353, 1995.

[7] N. A. Riza and N. Madamopoulos, " Photonic Time Delay Beamforming Architectures Using Polarization Switching Arrays," *SPIE Proc.*, Vol. 2754, Orlando, 1996.

[8] N. A. Riza, "Liquid crystal-based optical control of phased array antennas," *IEEE/OSA Journal of Lightwave Technology*, Vol. 10, No. 12, 1974-1984, 1992.

[9] N. A. Riza, "High optical isolation low loss moderate switching speed nematic liquid crystal optical switch," *Optics Letters*, Vol. 19, No.8, pp.1440-1447, 1994.

[10] N. A. Riza, "25-Channel nematic liquid crystal optical time-delay unit characterization," *IEEE Photonics Technology Letters*, Vol. 7, No. 11, 1285-1287, 1995.

[11] Displaytech Shutters User's manual, Version 1.1, February, 1994, Displaytech, Inc., Boulder, Colorado.

[12] Jinkee Kim and N. A. Riza, "Fiber Array Optical Coupling Design Issues for Photonic Beamformers," *SPIE Proc*, Vol. 2754, Orlando, April, 1996.

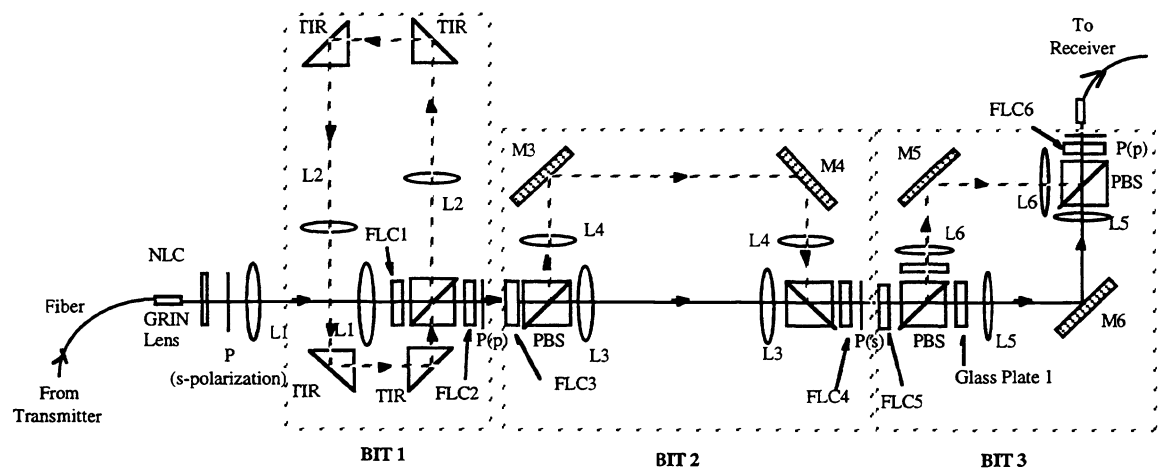


Fig.1 The experimental 3-bit PDL system using FLC devices, imaging optics, and fiber-optic remoting. The non-delay paths are represented with solid lines while the delay paths are represented with dashed lines.

Downloaded From: https://www.spiedigitallibrary.org/conference-proceedings-of-spie on 07 Jun 2020
Terms of Use: https://www.spiedigitallibrary.org/terms-of-use

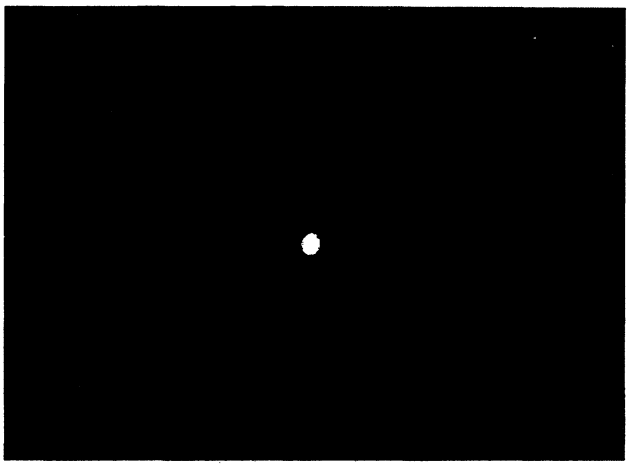


Fig.2 Image of the 1310 nm optical beam spot at the output plane of the PDL. The spot size is ~2 mm in diameter. The PDL input beam diameter was 1.8 mm.

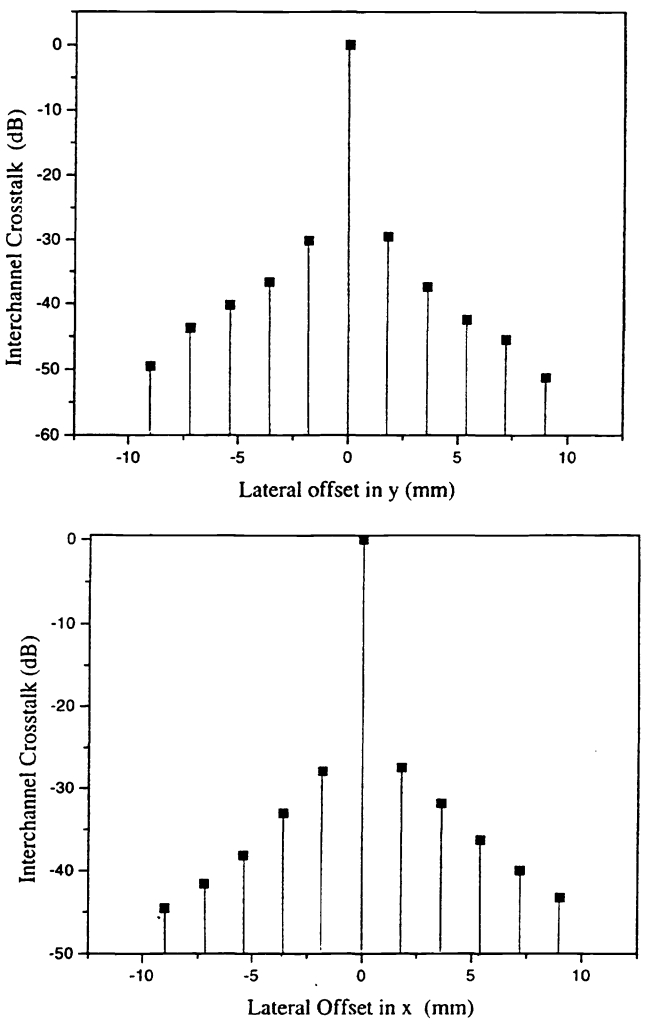
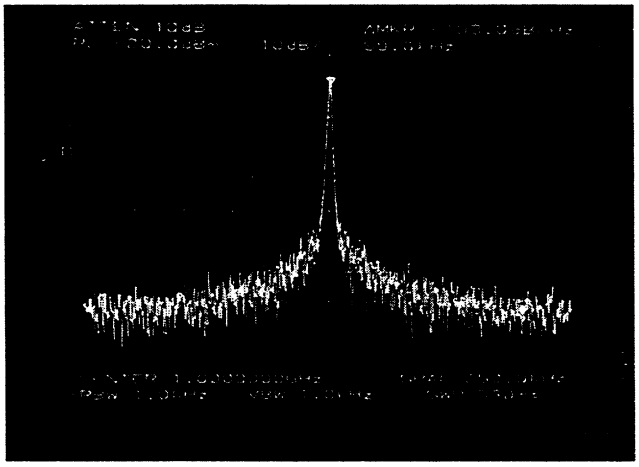


Fig.3 Optical interchannel crosstalk relative to the center active channel of the PDL, with measurements taken along the (a) x and (b) y directions at the PDL output plane. A maximum optical crosstalk of -27.47 dB (or - 54.94 dB rf) is measured at the nearest to center channel in the x-direction.

Downloaded From: https://www.spiedigitallibrary.org/conference-proceedings-of-spie on 07 Jun 2020
Terms of Use: https://www.spiedigitallibrary.org/terms-of-use

(a)



(b)

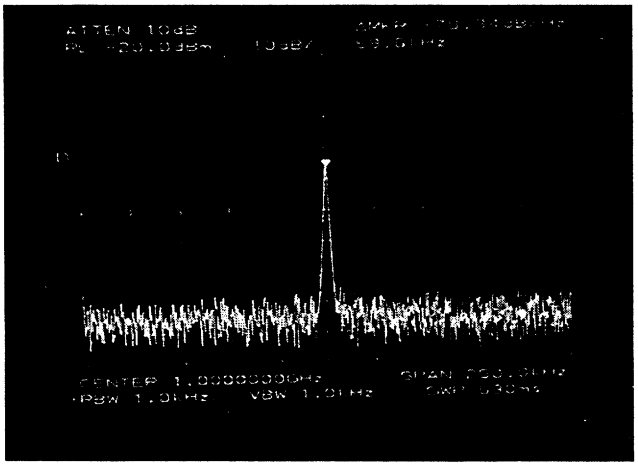


Fig.4. C/N measurements of the 1 Ghz modulation Lasertron QLINK1-051 fiber-optic link (a) without (103 dB/Hz) and (b) with (79.34 dB/Hz) the PDL, @ 100 Khz offset and analyzer RBW=1.0 kHz.

Downloaded From: https://www.spiedigitallibrary.org/conference-proceedings-of-spie on 07 Jun 2020
Terms of Use: https://www.spiedigitallibrary.org/terms-of-use

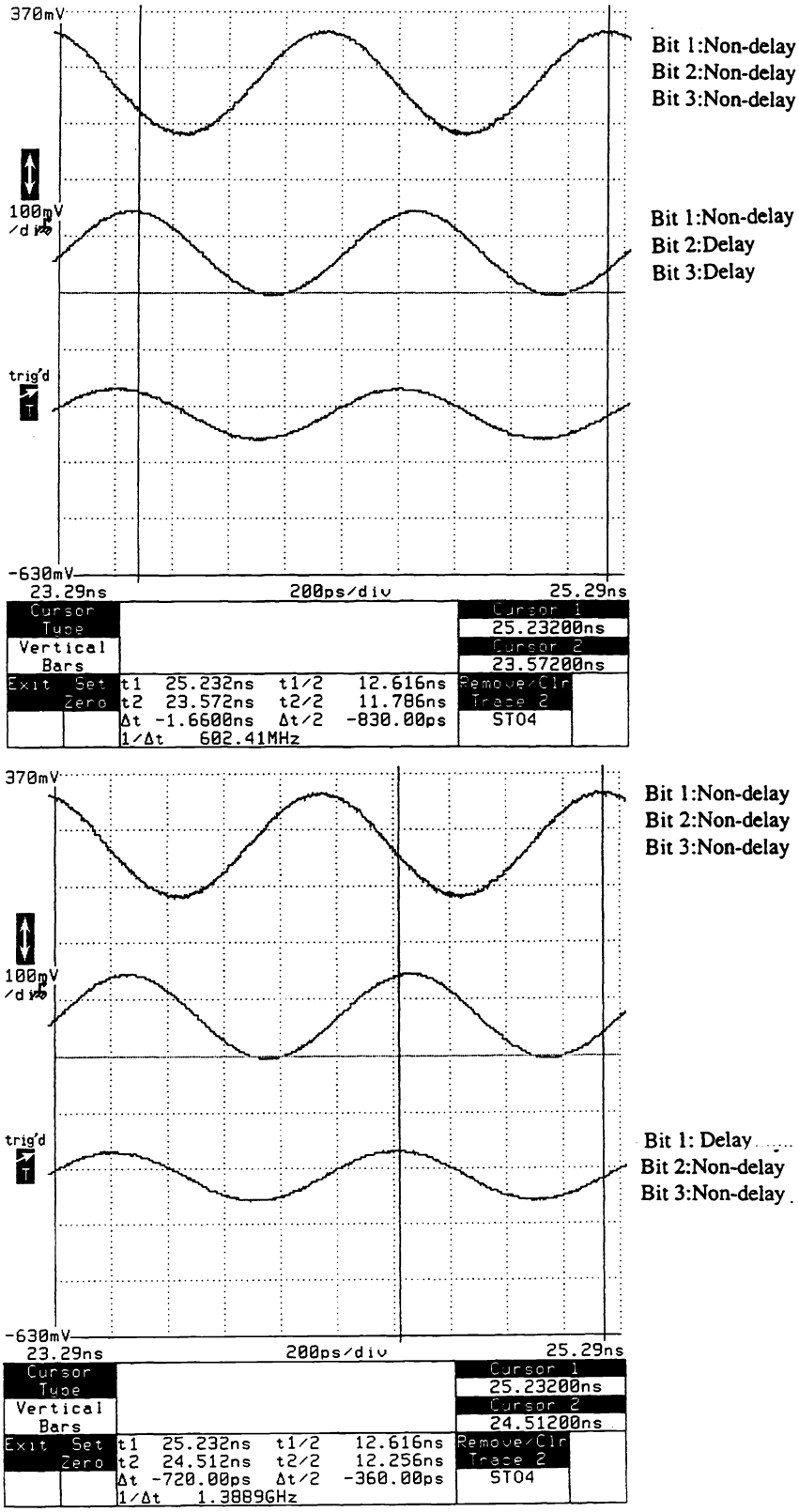


Fig.5 Oscilloscope traces showing the time delayed signals for three different time delay settings of the PDL. The top trace corresponds to the measured zero delay, the middle trace corresponds to a measured 1.660 ns delay, and the bottom trace corresponds to a 5.720 ns measured delay.

Downloaded From: https://www.spiedigitallibrary.org/conference-proceedings-of-spie on 07 Jun 2020
Terms of Use: https://www.spiedigitallibrary.org/terms-of-use

PDL Settings		Optical Loss Bit 1 (dB)	Optical Loss Bit 2 (dB)	Optical Loss Bit 3 (dB)	PDL Loss (dB)
1	Measured	Straight	Straight	Straight	
	Expected	2.40	1.67	1.49	5.56
		<2.50	< 1.87	< 2.00	< 6.47
2	Measured	Straight	Straight	Delay	
	Expected	2.40	1.67	1.37	5.44
		<2.50	< 1.87	< 2.00	< 6.47
3	Measured	Straight	Delay	Straight	
	Expected	2.40	1.61	1.49	5.5
		<2.50	< 2.00	< 2.00	< 6.47
4	Measured	Straight	Delay	Delay	
	Expected	2.40	1.61	1.37	5.38
		<2.50	< 2.00	< 2.00	< 6.47
5	Measured	Delay	Straight	Straight	
	Expected	5.5	1.67	1.49	8.66
		< 6.9	< 1.87	< 2.00	< 10.87
6	Measured	Delay	Straight	Delay	
	Expected	5.5	1.67	1.37	8.54
		< 6.9	< 1.87	< 2.00	< 10.87
7	Measured	Delay	Delay	Straight	
	Expected	5.5	1.61	1.49	8.6
		< 6.9	< 2.00	< 2.00	< 10.87
8	Measured	Delay	Delay	Delay	
	Expected	5.5	1.61	1.37	8.48
		< 6.9	< 2	< 2	< 10.87

Table 1. Measured and designed optical losses for each bit and for the overall PDL.

PDL Setting		Carrier-to-Noise ratio
1: Non-Delay 2: Non-Delay 3: Non-Delay	(Setting 1)	78.97 dB/Hz
1: Non-Delay 2: Non-Delay 3: Delay	(Setting 2)	77.17 dB/Hz
1: Non-Delay 2: Delay 3: Non-Delay	(Setting 3)	79.34 dB/Hz
1: Non-Delay 2: Delay 3: Delay	(Setting 4)	76.16 dB/Hz
1: Delay 2: Non-Delay 3: Non-Delay	(Setting 5)	67.17 dB/Hz

Table 2. C/N ratio measurements for five different time delay setting of the PDL. The measurements were obtained at a 100 kHz offset from the 1 Ghz carrier, using an analyzer resolution bandwidth of 1 Khz.

Downloaded From: https://www.spiedigitallibrary.org/conference-proceedings-of-spie on 07 Jun 2020
Terms of Use: https://www.spiedigitallibrary.org/terms-of-use